A Pressure Self-Adaptable Route for Uniform Lithium Plating and Stripping in Composite Anode

*Peng Shi, Xue-Qiang Zhang, Xin Shen, Bo-Quan Li, Rui Zhang, Li-Peng Hou, and Qiang Zhang**

Lithium (Li) metal anode confronts impressive challenges to revolutionize the current rechargeable batteries due to the intractably unstable interface. The composite Li anode is proposed to relieve volume fluctuations and suppress Li dendrites apparently. However, the inner space of composite anodes still affords feasibility for the continuous growth of unconstrained Li dendrites, leading to a low utilization of deposited Li and even safety hazards. Herein, an emerging and rational strategy to design composite anodes is proposed to regulate the inner Li plating/stripping. The self-adaptable pressure is generated by the filled elastic polymer inside conductive hosts, surpassing the yield strength of Li and confining Li to form a smooth morphology with a high utilization owing to the persistent electronic pathways under pressure. The pressure self-adaptable composite anode renders 160 cycles with a capacity retention of 80% in comparison to 60 cycles with a planar Li under practical conditions. Moreover, a 1.0 Ah pouch cell undergoes 68 cycles impressively. This work not only presents a fresh perspective on regulation of inner Li plating/stripping by introducing a self-adaptable pressure into the composite anode, but also demonstrates the avenue of exploring multifunctional composite anodes for practical Li metal batteries.

1. Introduction

High-energy-density storage technologies, such as cutting-edge rechargeable batteries, have attracted unprecedented research enthusiasm globally in order to meet the increasing demands of portable electronic devices, electric vehicles, and smart grids.[1] Lithium (Li)-ion battery is one of the most accentuated paradigms worldwide as acknowledged by the 2019 Nobel Prize in Chemistry.[2] However, the low theoretical specific capacity of graphite anode (372 mAh g^{-1}) in Li-ion battery limits its further applications.[3] Consequently, Li metal is reviving and attracts enormous interests nowadays as an excellent anode material due to its ultrahigh specific capacity (3860 mAh g^{-1}) and low reduction potential (−3.04 V vs standard hydrogen electrode).[4] However, Li metal anode is still not applied in practical rechargeable devices yet on account of the intrinsic bottlenecks, that is, uncontrolled Li dendrites and large volume fluctuations inducing unstable interface, which leads to a short lifespan and even safety hazards.[5]

In retrospect, tremendous efforts have been devoted to tackling the above issues and prolonging the lifespan of Li metal batteries (LMBs).[6] Extensive strategies focus on liquid electrolyte design,[7] artificial protective layers with high Young's modulus,[8] polymer or solid-state electrolytes,[9] and 3D hosts.[10] Particularly, the composite Li anode with a conductive 3D host can maintain a dimensional stability by confining Li deposition in the inside pores, exhibiting peculiar a merit in relieving volume fluctuations. Besides, the plentiful conductive surface significantly reduces the areal current density, diminishing the driven power of dendritic electrodeposition.[11] Unfortunately, the growth of Li dendrites in the confined space inside composite anode remains untouched which dictates the final lifespan of a battery cumulatively. The Li deposition inside a host can also lose electronic contacts and becomes the dead Li, which accumulates inside a host and then counteracts the expected role of a composite anode. Therefore, the innovative composite anodes are aspired to be explored with consideration of the inner Li plating/stripping in response to the challenges of practical conditions.

Recently, the inner behaviors of Li plating/stripping are also regulated by the lithiophilic layer of a 3D host, such as doped-nitrogen atom, metal oxide, and alloy layer, which have been comprehensively reported.[12] On the other hand, the mechanical methods are widely employed in protection of Li metal. For example, an artificial protective layer with high Young's modulus provides the desired mechanical strength to suppress the Li dendrite growth for a planar electrode during Li plating/stripping.[13] However, the methods which aptly make use of the mechanical properties of Li metal to regulate the inner Li plating/stripping in a composite anode are not touched yet.

In this contribution, an emerging and rational composite anode was freshly proposed by introducing a pressure self-adaptable route to regulate the inner behavior of Li plating/stripping inside the composite anode (**Figure 1**). In a routinely

---

P. Shi, X.-Q. Zhang, X. Shen, Dr. B.-Q. Li, Dr. R. Zhang, L.-P. Hou, Prof. Q. Zhang
Beijing Key Laboratory of Green Chemical Reaction Engineering and Technology
Department of Chemical Engineering
Tsinghua University
Beijing 100084, China
E-mail: zhang-qiang@mails.tsinghua.edu.cn

The ORCID identification number(s) for the author(s) of this article can be found under https://doi.org/10.1002/adfm.202004189.

DOI: 10.1002/adfm.202004189

© 2020 Wiley-VCH GmbH

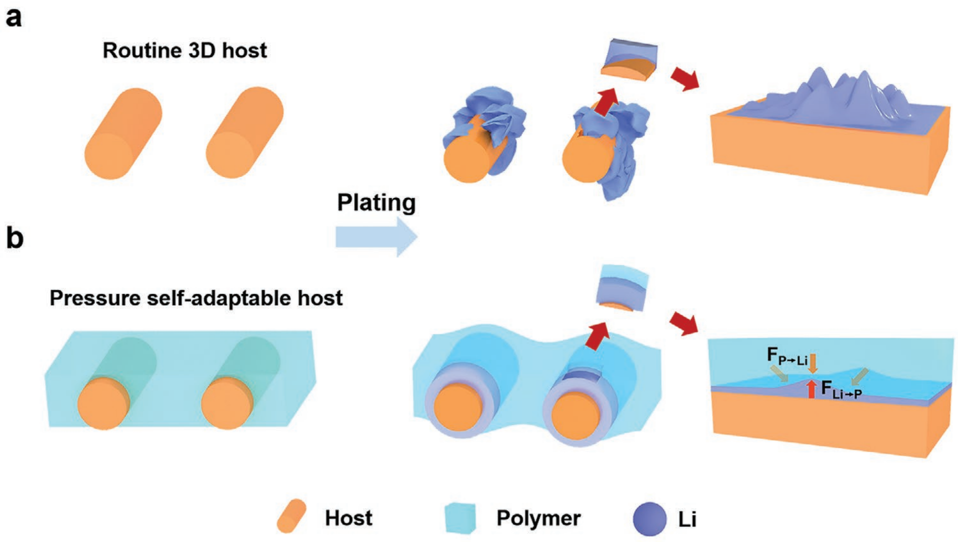

Figure 1. Schematic illustration of the plating process in composite anode with a) a routine 3D host and b) a pressure self-adaptable host. The Li dendrites always grow unimpededly on a routine host during the plating process. Once the elastic polymers are filled into the porous host, Li deposits on the conductive hosts, generating a compression force ($F_{\mathrm{Li} \rightarrow \mathrm{P}}$) to deform the filled polymer and then the induced force ($F_{\mathrm{P} \rightarrow \mathrm{Li}}$) is applied to the growing Li metal to render dense and smooth Li deposition.

conductive 3D host, Li dendrites can still grow unimpededly on the surface inside a host (Figure 1a). There is less room for Li metal to grow with freedom once the elastic polymers are filled into the host pores. The Li metal deposits on the conductive host during the plating process, generating a compression force ($F_{\mathrm{Li} \rightarrow \mathrm{P}}$) to deform the polymer (Figure 1b). As the displacements of polymer are restrained by host fibers, the elastic deformed polymer attempts to return to its initial state. Therefore, a normal stress ($F_{\mathrm{P} \rightarrow \mathrm{Li}}$) generates opposite to the direction of Li growth, which can be regarded as a pressure (P) on the growing Li metal. The applied pressure, which is larger than the yield strength of Li, has the ability to confine Li growth and plastically deform dendrites to maintain a dense and smooth morphology. During stripping, a high utilization of deposited Li is achieved owing to persistent electronic pathways between the deposited Li and a conductive host under pressure. A battery with a self-adaptable pressure composite Li anode exhibited a larger capacity retention of 80% after 160 cycles compared to a planar Li anode with 60 cycles. Additionally, a 1.0 Ah pouch cell underwent 68 cycles when it decreases to the 80% of initial capacity.

2. Results and Discussion

The feasibility of the composite anode with self-adaptable pressure bases on two prerequisites. On the one hand, the pressure generated by the polymer should be larger than the yield strength of Li deposition, which can suppress the uncontrolled growth of Li dendrites and smooth Li deposition. On the other hand, the deformation of filled polymer has to be in the elastic region to guarantee that the polymer takes effect during the whole repeated plating/stripping processes. Moreover, the strategy of self-adaptable pressure relies on the advantage of the 3D host, including abundant conductive area and slight volume fluctuation.

The finite element method was employed in order to clarify the pressure generated in composite anode precisely (**Figure 2**a). The pressure between the deposited Li and polymer can be up to 500 MPa when the deposited capacity of Li was 1.0 mAh cm^{-2}. The current density was based on planar electrode and polyacrylonitrile (PAN) was selected as a representative of polymers due to its great compatibility with Li metal. (Figure S1, Supporting Information). While the yield strength of both the micrometer-sized Li and bulk Li is less than 100 MPa, Li growth can be well confined through the permanent plastic deformation, leading to a more planar and smooth morphology on host fibers.[14] The self-adaptable pressure was also detected by a preliminary experiment. The change of pressure during Li plating was recorded in an electrolytic cell (Figure S2, Supporting Information). The self-adaptable pressure is approximately linear accompanying with Li plating (Figure S3, Supporting Information). Therefore, the boundary of the elastic polymer moves accompanying the deposited Li during the repeated plating/stripping processes (Figure 2b). The polymer shrinks inward with Li plating on the conductive hosts. Then the boundary (dash lines in right panel, Figure 2b) returns to the initial state (solid lines in left panel, Figure 2b) after Li stripping. The mechanical parameters and elastic deformation region of PAN are measured by nanoindentation to confirm whether PAN can perform the process described above (Figure S4, Supporting Information).[15] The Young's modulus of PAN maintains around 5.0 GPa from the initial state to a displacement of 2 µm which indicates that PAN undergoes elastic deformation rather than plastic deformation (Figure 2c).

In order to demonstrate the feasibility of self-adaptable pressure experimentally, copper (Cu) mesh was chosen due to the simple structure for observation (Figure S5, Supporting Information). The PAN was filled into the pores of Cu mesh to fabricate Cu mesh @ PAN (Figures S6 and S7, Supporting Information). There were many dendrites in pores of Cu mesh and

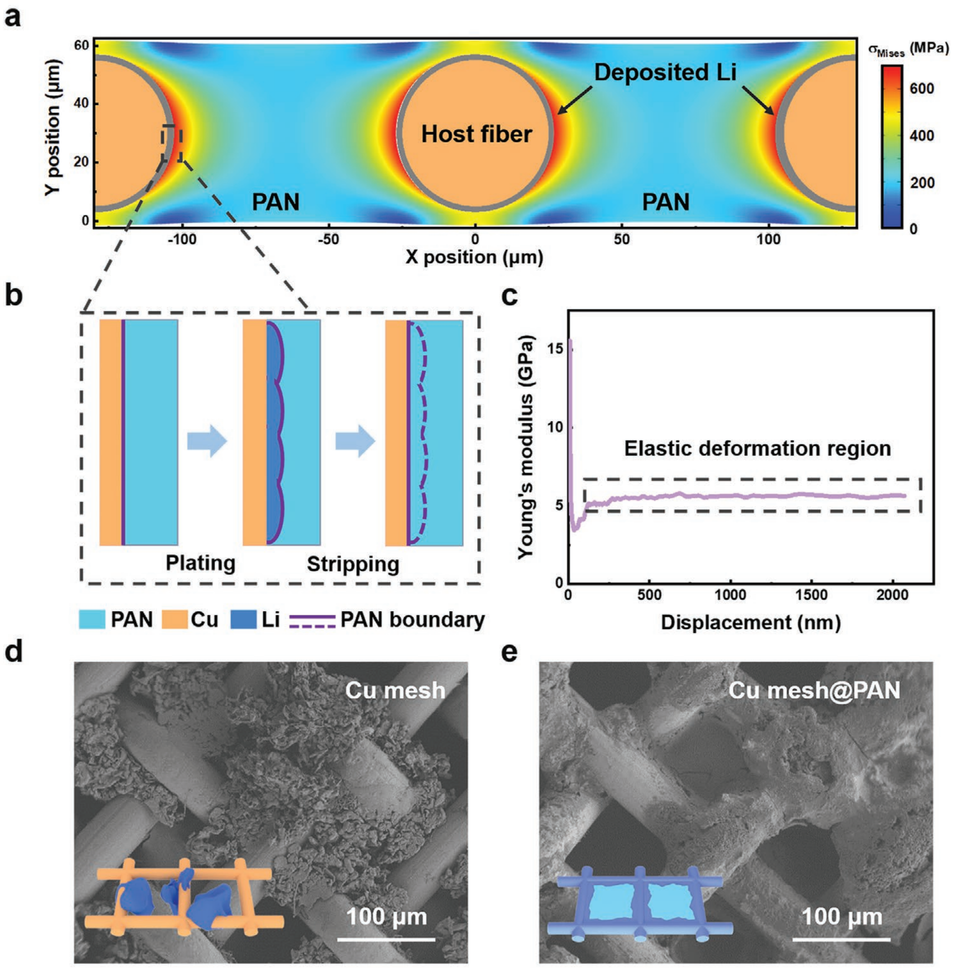

Figure 2. a) The distribution of von Mises stress in the host filled with PAN polymer during Li plating. b) Schematic illustration for the boundary displacement of PAN during Li plating and stripping. c) Young's modulus of PAN during the process of deformation. Top-view SEM images of d) Cu mesh and e) Cu mesh @ PAN after Li plating with a capacity of 1.0 mAh cm^{-2} at a current density of 1.0 mA cm^{-2}.

abundant protrusions on the surface of Cu fibers, performing inhomogeneous Li plating according to the scanning electron microscope (SEM) images (Figure 2d). In contrast, there is no obvious Li dendrites on the surface of Cu mesh @ PAN (Figure S8, Supporting Information) and the Li deposition on Cu mesh @ PAN was dense and smooth, which can be demonstrated obviously after removing the PAN from the surface (Figure 2e). The self-adaptable pressure stemming from the deformation of PAN on deposited Li contributes to regulating the behaviors of Li plating/stripping in confined space for a dense and smooth morphology of Li deposition. In a Li | Cu mesh @ PAN cell, the voltage profile exhibited no obvious difference with Cu mesh as an electrode during plating process with a hysteresis around 100 mV, indicating that the filled PAN did not block the transport of Li ions (Figure S9, Supporting Information). Additionally, Cu mesh @ PAN electrode had a higher Columbic efficiency (CE, 87.2%) than Cu mesh electrode (83.3%), proving that the deposited Li can be utilized more completely in Cu mesh @ PAN electrode. The dense deposited Li and persistent electronic pathways under the self-adaptable pressure afford a higher unitization efficiency of deposited Li.

The potential of pressure self-adaptable composite anode was further demonstrated under practical conditions after the proof-of-concept of that in Cu mesh host. Carbon fiber (CF) was employed as the 3D host due to the stable structure, appropriate specific surface area, and light weight (Figure S10a, Supporting Information).[16] The suitable specific surface area can increase the conductive specific surface area without consuming excessive electrolyte. The morphology and structure of CF@PAN anode were confirmed by the SEM and the energy dispersive spectroscopy (EDS) mapping. There was enough free space in the large pores of CF electrode for the continuous growth of Li dendrites, while the large pores were occupied by PAN in the CF@PAN anode (**Figure 3**a; Figure S10b, Supporting Information). The N element on the top surface indicates that PAN was distributed evenly in the host. The self-adaptable pressure derived from the deformation of the filled PAN during Li plating plastically deforms dendrites to maintain a dense and smooth morphology in CF@PAN.

3D X-ray microscopy (3D XRM) was employed for exploring the location of deposited Li in a practical system intuitively after the initial plating. The deposited Li, PAN, and CF can

© 2020 Wiley-VCH GmbH

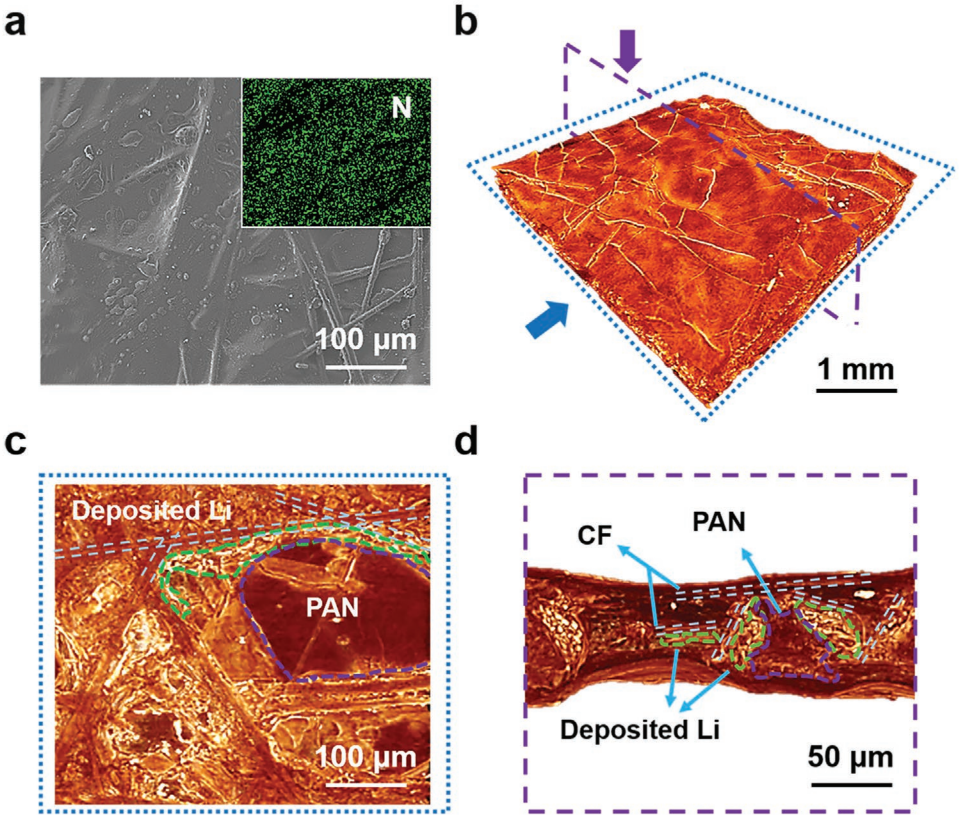

Figure 3. The surface morphology and structure of CF@PAN and the location of deposited Li in CF@PAN composite anode. a) Top-view SEM image of CF@PAN and EDS of the area in inset image. b) The 3D morphology of CF@PAN after Li plating by X-ray microscopy. c) The transverse section partial view along the blue dotted line in (b). d) The longitudinal section partial view along the purple dashed line in (b). The contrast of deposited Li is gloss white surrounded by green dotted line. The carbon fibers are distinct which are indicated by blue dash line and the PAN presents dark red surrounded by purple dotted line. (c) and (d) are the parts of the cross-sectional views of (b) in the arrow direction, respectively.

be distinguished obviously due to the different contrasts and shapes under 3D XRM images. There was no deposited Li on the surface of PAN and the PAN was not extruded from the pores after a high deposition areal capacity of 3.0 mAh cm^{-2}, which can meet the demand for practical batteries (Figure 3b). The deposited Li surrounded by green dotted line attached on CF and the other side was confined by PAN surrounded by purple dotted line, indicating that the deposited Li was along the conductive CF at the first stage (Figure 3c,d). Consequently, the self-adaptable pressure increases with the Li plating capacity and restrains the uncontrolled growth of Li. Furthermore, the morphology of Li plating/stripping was observed at the 10th cycle. The CF@PAN anode remained original structure, in which PAN was preserved and stable during the repeated Li plating/stripping processes (Figure S12, Supporting Information). The surface of CF@PAN anode was smooth and uniform differing from CF anode with numerous dendrites in the large pores with a capacity of 3.0 mAh cm^{-2} after the 10th plating (**Figure 4**a,b). There were few changes in the CF@PAN anode and the surface was still flat during the stripping process (Figure 4c). In contrast, considerable dead Li accumulated in the pores of CF due to the shaggy deposited Li and poor contacts between deposited Li and host fibers (Figure 4d). The deposited Li and CF were exposed after removing the PAN on the surface of CF@PAN electrode in order to further observe the morphology of Li plating/stripping. The deposited Li exhibited obvious deformation owing to being pressed in CF@PAN, indicating that the deposited Li was confined by the self-adaptable pressure (Figure S13a, Supporting Information). In this regard, the morphology of deposited Li in CF@PAN was similar to that observed on the planar Cu substrate in a pouch cell which was tested with an external pressure of 1.0 MPa (Figure S14, Supporting Information).[17] Additionally, the deposited Li stripped more completely and less dead Li remained in CF@PAN anode in comparison to CF anode (Figure S13b, Supporting Information). Therefore, the confined location and smooth morphology of the deposited Li in CF@PAN anode prove that the behaviors of Li plating/stripping in a self-adaptable composite anode can be regulated under practical conditions effectively.

Electrochemical impedance spectroscopy (EIS) measurements are applied to obtain the interfacial transport resistance of Li ions in Li/CF and Li/CF@PAN composite electrode. The interfacial resistance is the combination of the diffusion resistance of Li ion in the solid electrolyte interphase (SEI) layer (R_{SEI}) and the charge transfer resistance (R_{ct}). The much lower R_{SEI} and R_{ct} of the cell with Li/CF@PAN anode compared with the cell with Li/CF anode after repeated cycles suggest that the more stable Li ionic channel and less dead Li accumulation are achieved in Li/CF@PAN under the self-adaptable pressure during long cycles (Figure S15, Supporting Information). Owing to the low interfacial transport

© 2020 Wiley-VCH GmbH

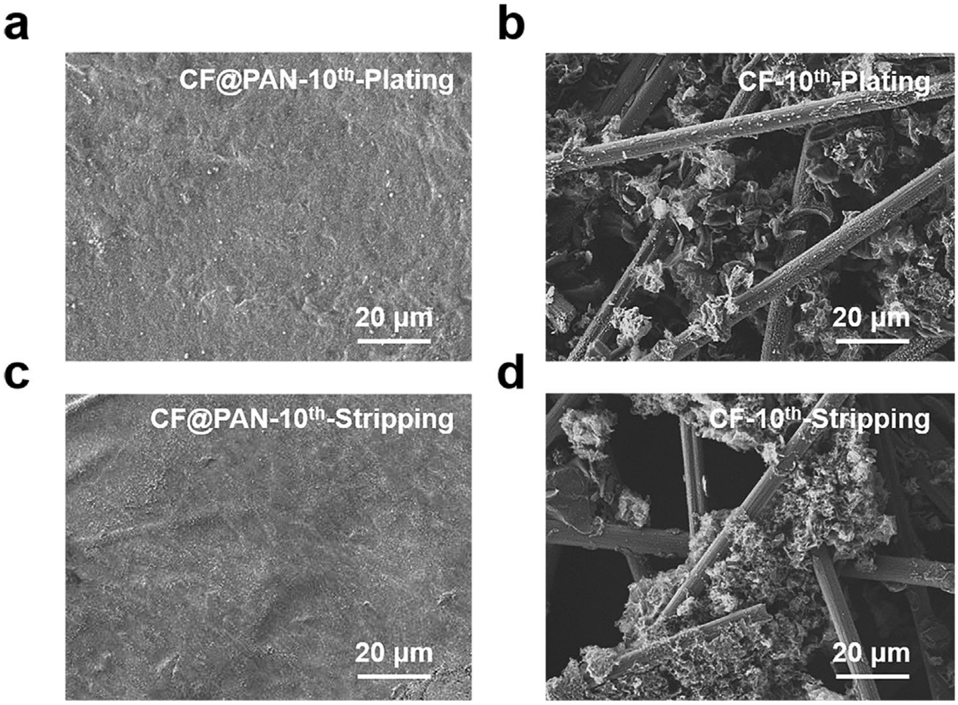

Figure 4. The morphology of the surface of composite anode during repeated cycling. Top-view SEM images of a,b) plating and c,d) stripping morphology for CF@PAN (a, c) and CF anode (b, d) after 10 cycles with a capacity of 3.0 mAh cm^{-2} at a current density of 1.0 mA cm^{-2}.

resistance of Li ions in Li/CF@PAN, a low hysteresis during repeated Li plating/stripping and superior stability are expected to be achieved in a full cell with Li/CF@PAN composite anode.

CE is an important parameter to evaluate the utilization of deposited Li in a composite anode for LMBs.[18] Herein the working electrode (CF@PAN) was pretreated in order to eliminate the loss associated with the side reactions between Li and hosts. The average CE over 50 cycles was 95% for CF@PAN electrode, higher than 91% for the planar electrode (Figure S16, Supporting Information). The host with a moderate specific surface area decreases the current density and leads to a uniform electric field which lowers the nucleation overpotential and renders uniform Li deposition. In addition, the CFs provide abundant electronic conductive pathways which decrease the resistance of electron transfer and the deposited Li closely contacts with the CFs under the self-adaptable pressure, ensuring the steady electronic pathway. The uniform deposition and persistent electronic pathways under the self-adaptable pressure ensure the high utilization of the deposited Li in CF@PAN anode.

Combining with a high loading $LiNi_{0.5}Co_{0.2}Mn_{0.3}O_2$ (NCM523) cathode, the full cell was assembled to further demonstrate the potential for practical applications of the self-adaptable composite anode. The Li/CF@PAN composite anode was fabricated by a facile method of rolling CF@PAN with ultrathin Li foil (33 μm), which was similar to the fabrication method of Li/CF composite anode.[19] Both a high capacity cathode (2.5 mAh cm^{-2}) and a low N/P ratio (≈2.6) were adopted in order to evaluate the composite anode under practical conditions. The capacity of the Li | NCM523 coin cell rapidly faded to 80% retention after 60 cycles at 0.4 C (**Figure 5**a). Undoubtedly, the cycle performance of the Li/CF | NCM523 cell was better than planar Li, which can achieve 110 cycles under the benchmark of 80% capacity retention. In contrast, Li/CF@PAN | NCM523 coin cell exhibited better cycling stability than Li | NCM523 and Li/CF | NCM523 cells. The Li/CF@PAN | NCM523 maintained 80% of capacity retention for 160 cycles with a reduced polarization (Figure 5b). All fresh Li was pulverized and enormous dead Li were on the surface of planar Li anode after 100 cycles (Figure S17a, Supporting Information). In contrast, the surface was still flat for Li/CF@PAN anode after 200 cycles, illustrating the sturdiness of Li/CF@PAN composite anode and validating that the PAN maintain stable in contact with Li metal over many cycles (Figure S17b, Supporting Information). No dead Li or dendritic Li was observed on the surface of composite anode toward separator. Additionally, the chunks of Li can be observed on the side of back to the separator after 200 cycles (Figure S18, Supporting Information). The uniform plating and stripping are achieved in the Li/CF@PAN composite anode, which maintains the persistent electronic pathway between deposited Li and host, thus resulting in the enhance of the utilization efficiency of Li metal. The Li-free full cell with a CF@PAN anode can achieve stable performance over 30 cycles but the capacity of Cu | NCM523 cell rapidly decayed after 10 cycles, which further indicates the uniform Li plating/stripping and high utilization of deposited Li in the CF@PAN anode (Figure S19, Supporting Information).

Moreover, Li@PAN was employed to evaluate the effect of self-adaptable pressure for planar electrodes. The full cell with Li@PAN anode performed 90 cycles when the capacity decayed to 80% of initial capacity (Figure 5a). The deposited Li was inhomogeneous at the 10th plating and considerable dead

© 2020 Wiley-VCH GmbH

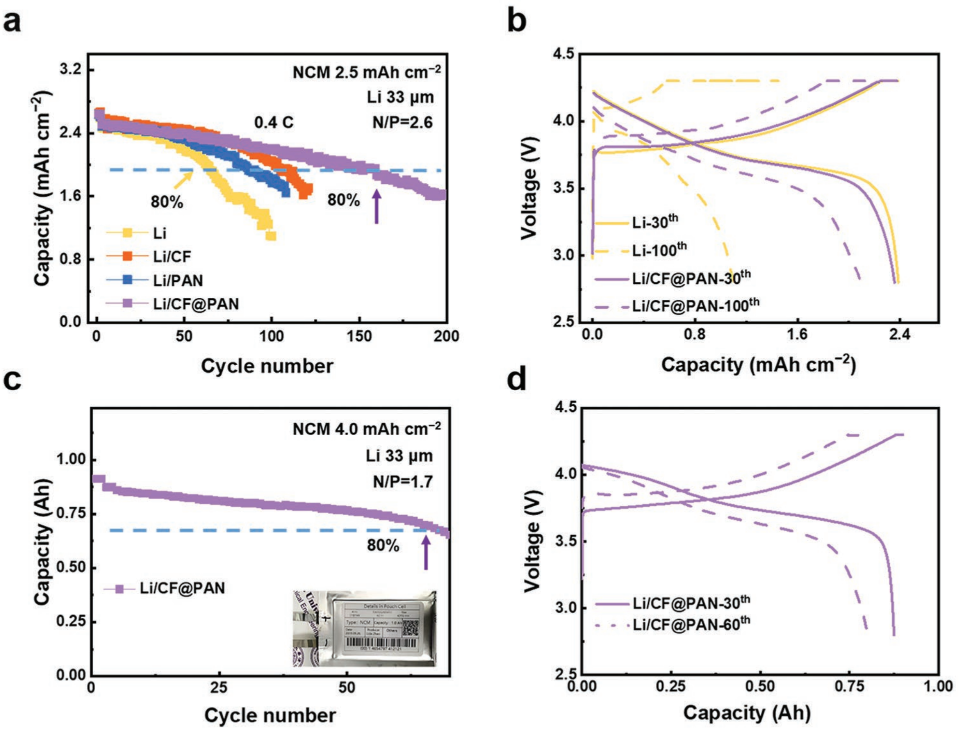

Figure 5. The cycling performance of full batteries under practical conditions. a) The cycling performance of coin cells with NCM 523 cathode and different anodes at 0.4 C. b) The corresponding voltage profiles of coin cells at the 30th and 100th cycle with planar Li and Li/CF@PAN anode. c) The cycling performance of a 1.0 Ah pouch cell at 0.1 C and the digital image of the pouch cell is inserted. d) The voltage-capacity profiles of a pouch cell at the 30th and 60th cycles.

Li were observed on the surface of Li@PAN (Figure S20, Supporting Information). The PAN on the surface of planar electrode undergoes plastic yielding or even ruptures due to a much greater volume change than the 3D composite anode with the same cycle capacity, and thus losing its regulation on behaviors of Li plating/stripping, which indicates the strategy relies on the 3D host with abundant effective electrochemical active area.

The Li/CF@PAN composite anode matching with higher areal loading cathode of 4.0 mAh cm^{-2} was further employed in coin and pouch cells to evaluate the potential of the novel design strategy (The specifications of the pouch cell are exhibited in Table S2, Supporting Information).[20] The full coin cell with a high areal loading cathode of 4.0 mAh cm^{-2} can achieve 70 cycles when the capacity declined to 80% (Figure S21, Supporting Information). The first discharge capacity of the pouch cell was 0.91 Ah and 68 cycles were achieved in a Li/CF@PAN | NCM523 pouch cell at 0.1 C with a minor polarization (Figure 5c,d). The self-adaptable composite anode prominently regulates the behaviors of Li plating/stripping and contributes to the stability of the Li pouch cell, which is of great significance for practical applications.

3. Conclusion

An emerging pressure self-adaptable strategy is proposed to regulate the behaviors of Li plating/stripping in a composite Li anode in response to the challenges from practical LMBs. The importance of inner Li plating/stripping in confined space was investigated, which strengthens the understanding of the electrochemical behavior of Li metal inside composite anode at micrometer scale. Moreover, the pattern of the Li behaviors disclosed under the self-adaptable pressure further contributes to exploring mechanism of coupled electrochemo-mechanics during Li plating/stripping. The self-adaptable pressure originates from the deformation of the elastic polymer inside composite anode and changes with the increased Li deposition. The self-adaptable pressure is larger than the yield strength of deposited Li, which confines the deposited Li in dense and smooth morphology. Therefore, a high utilization of deposited Li and then less dead Li are achieved due to the smooth Li and persistent electronic pathways under the self-adaptable pressure. The self-adaptable composite anode in a full battery exhibited a high capacity retention of 80% after 160 cycles, threefold lifespan than that of planar Li anode (60 cycles) under practical conditions. Additionally, a pouch cell underwent 68 cycles based on 80% capacity retention. This work demonstrates the potential of self-adaptable pressure on the regulation of Li plating/stripping inside composite anode toward practical challenges. The universal and rational route sets a great example in developing multifunctional composite anodes for long-lifespan rechargeable batteries.

Supporting Information

Supporting Information is available from the Wiley Online Library or from the author.

Acknowledgements

This work was supported by National Key Research and Development Program (2016YFA0202500), National Natural Science Foundation of China (21825501, 21805161, and U1801257), and the Tsinghua University Initiative Scientific Research Program.

Conflict of Interest

The authors declare no conflict of interest.

Keywords

composite anodes, lithium metal batteries, self-adaptable pressure, uniform lithium plating

Received: May 14, 2020
Revised: September 15, 2020
Published online:

---

[1] X. B. Cheng, R. Zhang, C. Z. Zhao, Q. Zhang, *Chem. Rev.* **2017**, *117*, 10403.

[2] H. Zhang, C. Li, G. G. Eshetu, S. Laruelle, S. Grugeon, K. Zaghib, C. Julien, A. Mauger, D. Guyomard, T. Rojo, N. Gisbert-Trejo, S. Passerini, X. Huang, Z. Zhou, P. Johansson, M. Forsyth, *Angew. Chem., Int. Ed.* **2020**, *59*, 534.

[3] S. H. Jiao, J. M. Zheng, Q. Y. Li, X. Li, M. H. Engelhard, R. G. Cao, J. G. Zhang, W. Xu, *Joule* **2018**, *2*, 110.

[4] W. Xu, J. L. Wang, F. Ding, X. L. Chen, E. Nasybutin, Y. H. Zhang, J. G. Zhang, *Energy Environ. Sci.* **2014**, *7*, 513.

[5] a) P. Shi, X. B. Cheng, T. Li, R. Zhang, H. Liu, C. Yan, X. Q. Zhang, J. Q. Huang, Q. Zhang, *Adv. Mater.* **2019**, *31*, 1902785; b) Y. He, X. Ren, Y. Xu, M. H. Engelhard, X. Li, J. Xiao, J. Liu, J. G. Zhang, W. Xu, C. Wang, *Nat. Nanotechnol.* **2019**, *14*, 1042.

[6] a) D. P. Lv, Y. Y. Shao, T. Lozano, W. D. Bennett, G. L. Graff, B. Polzin, J. G. Zhang, M. H. Engelhard, N. T. Saenz, W. A. Henderson, P. Bhattacharya, J. Liu, J. Xiao, *Adv. Energy Mater.* **2015**, *5*, 1402290; b) Y. Zhao, Y. Ye, F. Wu, Y. Li, L. Li, R. J. Chen, *Adv. Mater.* **2019**, *31*, 1806532; c) K. Yan, J. Y. Wang, S. Q. Zhao, D. Zhou, B. Sun, Y. Cui, G. X. Wang, *Angew. Chem., Int. Ed.* **2019**, *58*, 11364; d) A. J. Louli, J. Li, S. Trussler, C. R. Fell, J. R. Dahn, *J. Electrochem. Soc.* **2017**, *164*, A2689.

[7] a) K. Xu, *Chem. Rev.* **2004**, *104*, 4303; b) X. Fan, L. Chen, O. Borodin, X. Ji, J. Chen, S. Hou, T. Deng, J. Zheng, C. Yang, S.-C. Liou, K. Amine, K. Xu, C. Wang, *Nat. Nanotechnol.* **2018**, *13*, 715.

[8] a) R. Xu, Y. Xiao, R. Zhang, X. B. Cheng, C. Z. Zhao, X. Q. Zhang, C. Yan, Q. Zhang, J. Q. Huang, *Adv. Mater.* **2019**, *31*, 1808392; b) X. Liang, Q. Pang, I. R. Kochetkov, M. S. Sempere, H. Huang, X. Sun, L. F. Nazar, *Nat. Energy* **2017**, *2*, 17119.

[9] a) C. Z. Zhao, P. Y. Chen, R. Zhang, X. Chen, B. Q. Li, X. Q. Zhang, X. B. Cheng, Q. Zhang, *Sci. Adv.* **2018**, *4*, eaat3446; b) M. D. Tikekar, L. A. Archer, D. L. Koch, *Sci. Adv.* **2016**, *2*, e1600320; c) I. Aldalur, M. Martinez-Ibañez, M. Piszcz, H. Zhang, M. Armand, *Batteries Supercaps* **2018**, *1*, 149.

[10] a) C. Niu, H. Pan, W. Xu, J. Xiao, J. G. Zhang, L. Luo, C. Wang, D. Mei, J. Meng, X. Wang, Z. Liu, L. Mai, J. Liu, *Nat. Nanotechnol.* **2019**, *14*, 594; b) L. Chen, X. Fan, X. Ji, J. Chen, S. Hou, C. Wang, *Joule* **2019**, *3*, 732; c) W. D. Zhang, H. L. L. Zhuang, L. Fan, L. N. Gao, Y. Y. Lu, *Sci. Adv.* **2018**, *4*, eaar4410; d) Q. Song, H. B. Yan, K. D. Liu, K. Y. Xie, W. Li, W. H. Gai, G. H. Chen, H. J. Li, C. Shen, Q. G. Fu, S. Y. Zhang, L. L. Zhang, B. Q. Wei, *Adv. Energy Mater.* **2018**, *8*, 1800564; e) W. Deng, W. Zhu, X. Zhou, X. Peng, Z. Liu, *ACS Appl. Mater. Interfaces* **2018**, *10*, 20387.

[11] a) S. Jin, Y. Jiang, H. Ji, Y. Yu, *Adv. Mater.* **2018**, *30*, 1802014; b) C. Zhang, A. Wang, J. Zhang, X. Guan, W. Tang, J. Luo, *Adv. Energy Mater.* **2018**, *8*, 1802833; c) S. Liu, A. X. Wang, Q. Q. Li, J. S. Wu, K. V. Chiou, J. X. Huang, J. Y. Luo, *Joule* **2018**, *2*, 184; d) R. Zhang, X. B. Cheng, C. Z. Zhao, H. J. Peng, J. L. Shi, J. Q. Huang, J. F. Wang, F. Wei, Q. Zhang, *Adv. Mater.* **2016**, *28*, 2155.

[12] a) C. P. Yang, Y. Yao, S. He, H. Xie, E. Hitz, L. B. Hu, *Adv. Mater.* **2017**, *29*, 1702714; b) F. Liu, R. Xu, Z. Hu, S. Ye, S. Zeng, Y. Yao, S. Li, Y. Yu, *Small* **2019**, *15*, 1803734; c) G. H. Yang, J. D. Chen, P. T. Xiao, P. O. Agboola, I. Shakir, Y. X. Xu, *J. Mater. Chem. A* **2018**, *6*, 9899; d) B. Q. Li, X. R. Chen, X. Chen, C. X. Zhao, R. Zhang, X.-B. Cheng, Q. Zhang, *Research* **2019**, *2019*, 4608940; e) R. Pathak, Y. Zhou, Q. Qiao, *Appl. Sci.* **2020**, *10*, 4185.

[13] a) R. Pathak, K. Chen, A. Gurung, K. M. Reza, B. Bahrami, J. Pokharel, A. Baniya, W. He, F. Wu, Y. Zhou, K. Xu, Q. Q. Qiao, *Nat. Commun.* **2020**, *11*, 93; b) R. Pathak, K. Chen, A. Gurung, K. M. Reza, B. Bahrami, F. Wu, A. Chaudhary, N. Ghimire, B. Zhou, W. H. Zhang, Y. Zhou, Q. Q. Qiao, *Adv. Energy Mater.* **2019**, *9*, 1901486.

[14] a) V. Yurkiv, T. Foroozan, A. Ramasubramanian, R. Shahbazian-Yassar, F. Mashayek, *MRS Commun.* **2018**, *8*, 1285; b) C. Xu, Z. Ahmad, A. Aryanfar, V. Viswanathan, J. R. Greer, *Proc. Natl. Acad. Sci. USA* **2017**, *114*, 57; c) X. Wang, W. Zeng, L. Hong, W. Xu, H. Yang, F. Wang, H. Duan, M. Tang, H. Jiang, *Nat. Energy* **2018**, *3*, 227.

[15] Y. W. Chen Yang, Y. T. Chen, H. C. Chen, W. T. Lin, C. H. Tsai, *Polymer* **2009**, *50*, 2856.

[16] a) Y. Zhou, Y. Han, H. Zhang, D. Sui, Z. Sun, P. Xiao, X. Wang, Y. Ma, Y. Chen, *Energy Storage Mater.* **2018**, *14*, 222; b) T. T. Zuo, X. W. Wu, C. P. Yang, Y. X. Yin, H. Ye, N. W. Li, Y. G. Guo, *Adv. Mater.* **2017**, *29*, 1700389.

[17] a) A. J. Louli, M. Genovese, R. Weber, S. G. Hames, E. R. Logan, J. R. Dahn, *J. Electrochem. Soc.* **2019**, *166*, A1291; b) A. S. Mussa, M. Klett, G. Lindbergh, R. W. Lindström, *J. Power Sources* **2018**, *385*, 18.

[18] B. D. Adams, J. M. Zheng, X. D. Ren, W. Xu, J. G. Zhang, *Adv. Energy Mater.* **2018**, *8*, 1702097.

[19] P. Shi, T. Li, R. Zhang, X. Shen, X. B. Cheng, R. Xu, J. Q. Huang, X. R. Chen, H. Liu, Q. Zhang, *Adv. Mater.* **2019**, *31*, 1807131.

[20] C. Niu, H. Lee, S. Chen, Q. Li, J. Du, W. Xu, J. G. Zhang, M. S. Whittingham, J. Xiao, J. Liu, *Nat. Energy* **2019**, *4*, 551.

© 2020 Wiley-VCH GmbH